MEASUREMENTS OF AC LOSS IN CORED Nb_3Sn RUTHERFORD CABLES: INTERSTRAND CONTACT RESISTANCE AS FUNCTION OF CORE WIDTH

Cite as: AIP Conference Proceedings **986**, 285 (2008); https://doi.org/10.1063/1.2900358
Published Online: 04 March 2008

E. W. Collings, M. D. Sumption, E. Barzi, et al.

AIP Conference Proceedings **986**, 285 (2008); https://doi.org/10.1063/1.2900358

MEASUREMENTS OF AC LOSS IN CORED Nb_3Sn RUTHERFORD CABLES: INTERSTRAND CONTACT RESISTANCE AS FUNCTION OF CORE WIDTH

E.W. Collings[1], M.D. Sumption[1] , E. Barzi[2], D. Turrioni[2], R. Yamada[2], A.V. Zlobin[2], Y. Ilyin[3], and A. Nijhuis[3]

[1] Laboratories for Applied Superconductivity and Magnetism (LASM), MSE Dept, The Ohio State University, Columbus OH 43210, USA

[2] Fermi National Accelerator Laboratory, Batavia, IL 60510, USA

[3] Low Temperature Division, Faculty of Applied Physics, University of Twente, Enschede, NL

ABSTRACT

Magnetic measurements of cored-cable AC loss accompanied by SEM measurements of cable cross sections have been made in an investigation of the effects of core width and position on the effective interstrand contact resistance, $R_{\perp,eff.}$. The results were compared with those of previous studies of Rutherford cables with cores of various widths and designs. It was noted that although the uncored $R_{\perp,eff.}$s agreed well with those measured previously the cored results fell short of expectation. The suppression of $R_{\perp,eff.}$ is attributed to several factors that differ from cable to cable: e.g. displacement of the narrower cores to one edge of the cable, shrinkage in the width of the widest core as a result of severe compaction-induced imprinting. After allowing for these factors the projected $R_{\perp,eff.}$ tended to agree with previous results for full-width-core Nb_3Sn cables.

Keywords: Nb_3Sn, critical frequency, AC loss, contact resistance
PACs: 74.25 Ha, 74.25 Nf, 74.70 Ad, 84.71 Fk

INTRODUCTION

The design and fabrication of Nb_3Sn quadrupoles magnets is ongoing in the US under the inter-laboratory LHC Accelerator Research Program, LARP. Although not directly part of LARP, but nevertheless supportive of its goals, is a research collaboration established between OSU's Laboratory for Applied Superconductivity and Magnetism (LASM) and the Fermi National Accelerator Laboratory (FNAL) – with help from the University of Twente's Low Temperature Division -- for studying the properties of Nb_3Sn strands and cables. Of particular interest are the stability, AC loss, and interstrand contact resistance, ICR, of Nb_3Sn cables with cores. In order to ensure stability and to reduce distortions of the cable-wound dipoles it is important to control the magnitudes of

CP986, *Advances in Cryogenic Engineering: Transactions of the International Cryogenic Materials Conference - ICMC, Vol. 54,* edited by U. Balachandran

interstrand coupling currents (ICC) and "supercurrents" [1] (or boundary-induced coupling currents, BICCs [2]). The suppression of ICC currents with increasing ICR is well known. While the situation is more complicated for BICCs, ICR increases generally suppress these as well (see specifically the results in [2], pp 140-1 and preceding work, where resistive cores are shown to reduce BICCs by about an order of magnitude). Thus, both of these are suppressed by *increasing* the cables' crossover and side-by-side ICRs, $R_{\perp}$ and $R_{//}$, respectively, but to the detriment of current sharing and hence stability. A compromise between ICC and BICC reduction and magnet stability is required. From AC loss and field quality considerations, it can be shown that $R_{//}$ should not be not less than 0.2 μΩ [2] and that $R_{\perp}$ should be about 15±5 μΩ [3]. These latter numbers were specifically advanced for the LHC, but will be comparable for similar aspect ratio cables whether they are NbTi based or Nb_3Sn based. On the other hand, the ICR values should not be too high otherwise stability will be degraded, although no hard numbers seem to be available. The introduction of a stainless steel core into the Nb_3Sn-wound cable assists in the attainment of these goals.

Numerous studies have been made on cored Rutherford cables beginning with the pioneering experiments of Yamada et al [4] and continuing (starting in the mid-1990s) with studies by the LASM group of cored cables wound with bare-NbTi, stabrite-coated NbTi, Nb_3Al, Bi:2212, and Nb_3Sn strands, e.g. [5]. In retrospect it is clear that bare-Cu-stabilized NbTi cables cured at 225-250°C and stabrite-coated NbTi/Cu cables cured at 200°C were good models for the 650°C-RHTd uncored Nb_3Sn cables to come, in that interstrand diffusion bonding guaranteed in all cases very small $R_{\perp}$ values. As pointed out in [6] there are several ways of coating the surfaces of NbTi- and Nb_3Sn strands to control the ICRs of cables wound from them. The inclusion of a core provides another mechanism. For this reason a series of studies was initiated on the influence of cores with various thicknesses and widths on the ICRs of stabrite-coated LHC-class NbTi cables [7][8], followed by AC loss measurements of Nb_3Sn cables provided with cores of various kinds and thicknesses: simple 25μm thick AISI316 stainless steel tape [9], double-bimetallic and composite SS/Cu tapes [10]. But this report represents the first of a series of studies of the influence of *cabling-compaction* and *core width* on the AC loss on Nb_3Sn cables. Here we report on the results of magnetic measurements of AC loss in cables with stainless cores of nominal widths 10.8, 5.2, and 4.5 mm comparing them with that of an uncored cable and show how the desired $R_{\perp} = 15\pm5$ μΩ can be approached by increasing the width of the core.

SAMPLE MATERIALS AND PREPARATION

In preparation for this study FNAL wound many tens of meters of 27-strand Rutherford cable using 1 mm diameter RRP Nb_3Sn-precursor strand from Oxford Superconducting Technologies (OST). Stainless steel strips (AISI316, 25 μm thick) of widths 4.5, 5.2, and 10.8 mm were introduced in succession during the winding. At LASM, four sets each of five cable segments 20 inches long were wrapped with S-glass tape (about 25% overlap) in readiness for the assembly of four 5-high cable packs. Each set of five cable segments was stacked into a stainless steel fixture designed to apply side-constraint during uniaxial compression, after which the following operations were

performed at FNAL: (1) A ceramic-precursor solution was squirted onto the exposed edges of the cable packs, following which uniaxial pressure of 35 MPa was applied in a hydraulic press and secured by tightening down the fixture nuts. (2) The insulation was then cured for 30 min/150°C (plus up- and down ramps) and the pressure released. (3) The assemblies were then returned to the hydraulic press, compacted to 10 MPa and re-bolted. (4) In a sealed flowing-Ar retort the assemblies experienced 72h/210°C + 48h/400°C + 48h/650°C interspersed with ramps of 50°C/h, a heat-treatment specification intended to provide a combination of high J_c and RRR. After being shipped back to LASM the cable packs were: (1) removed from the RHT fixture, wrapped in teflon film, installed in silicone-greased aluminum molds, uniaxially loaded and retained at 10 MPa, (2) vacuum impregnated with CTD-101 resin, cured following CTD's standard recommendations, and cut to a length of 396 mm in readiness for AC loss measurement.

TABLE 1. Details of the Cable Samples for AC Loss Measurement.

The Strand	
Type	OST-RRP Billet No. 8853-2616
Diam, mm	1.0
Filament count	60/(61) subelements spaced 50% more than in the standard array
Filament diam., μm	~100
The Cables	
Strand count, *N*	27
Keystone angle, deg.	0.95
Level of compaction, %	87
Width, *w*, mm	14.23
Thickness (av.), *t*, mm	1.78 (hence aspect ratio, $w/t = 7.99$)
Transposition pitch, 2*Lp*, mm	110.2
Insulation	S-glass tape wrap/CTD-101 resin
Core type	AISI316, 25 μm thick
Cable No./Core width (mm)	Cable 3/NC, Cable 4/4.5, Cable 5/5.2, Cable 6/10.8

MAGNETIC MEASUREMENT OF AC LOSS

The principal components of a Rutherford cable's total per-cycle loss, $Q_t(f)$, are: (i) the strand's "persistent current" magnetization loss, Q_h, (ii) its relatively negligible eddy current loss, $Q_e(f)$, and (iii) the cable's frequency dependent coupling loss, $Q_c(f)$. Magnetic measurements of $Q_t(f) = Q_h + Q_c(f)$ were made at 4.2 K using the inductive- or pick-up-coil method on the same samples mounted inside the University of Twente's calorimeter/magnetometer [11]. The loss was generated by transverse AC fields of amplitude $B_m = 400$ mT and frequencies, f, of up to 80 mHz except that Cable 6 received a second measurement at $B_m = 50$ mT with f up to 1000 mHz. The magnetic loss was calibrated against the calorimetric loss of one of the cable packs at a selected frequency, the calorimeter having been calibrated against ohmic loss developed in a built-in 100 Ω resistor.

Measurements of $Q_t(f)$ in the face-on (FO) direction of the applied field yielded a coupling loss designated $Q_\perp(f)$ after a weakly linear base-line with intercept $Q_h = Q_t(f \to 0)$ (the latter from a parallel set of calorimetric measurements) had been subtracted.

AC LOSS DETERMINATION OF ICR

Low Frequency AC Loss – The Initial-Slope Method

The per-cycle coupling current loss, $Q_{\perp}(f)$, can be usefully expressed in terms of the following expression based on calculations by Sytnikov et al. [12]:

$$Q_{\perp} = \left(\frac{2\pi^2}{3}\right)\left(\frac{w}{t}\right)L_p B_m^2\left[\frac{N^2}{20R_{\perp}} + \frac{1}{NR_{\parallel}}\right].f \qquad (1)$$

where w/t is the width/thickness aspect ratio of an N-strand cable, L_p (in m) is one-half of the transposition pitch, B_m (in T) is the amplitude of an applied field oscillating at a frequency f, $R_{\perp}$ is the cross-over, and $R_{//}$ the side-by-side ICRs (in Ω). For uncored cables such that $R_{\perp} \quad (1/20)N^3R_{//}$ the latter can be neglected in Equation (1). On the other hand in cored cables, especially when variable width needs to be considered, it is preferable to combine the FO ICRs into an "effective value " defined by:

$$Q_{\perp} = \left(\frac{2\pi^2}{3}\right)\left(\frac{w}{t}\right)L_p B_m^2\left[\frac{N^2}{20R_{\perp,eff.}}\right].f \quad \text{in which} \quad \frac{1}{R_{\perp,eff.}} = \frac{1}{R_{\perp}} + \left(\frac{20}{N^3}\right)\frac{1}{R_{\parallel}} \qquad (2)$$

As shown in a series of earlier papers [5,7,8,9,10] on the effects of cores in NbTi and Nb_3Sn superconductor based cables, it is frequently the case that the resistivity of the cores is dominated by the oxide surfaces that form on them, such that the actual value of $R_{\perp}$ is quite high. For example the coupling current loss is nearly negligible in the cored cables of ref [9], indicating the existence of a very high $R_{\perp}$. In some cases [9] the values of $R_{//}$ are not sufficiently low to contribute much to the loss, but in other cases (especially for NbTi based cables), they can dominate the creation of loss in even the perpendicular field orientation [10]. The dominance of $R_{//}$ influences on perpendicular field loss was investigated in detail for NbTi based cables in [13]. However, from a magnet engineering point of view, it is usually more useful to discuss this loss, whether it comes fully from $R_{//}$-related paths, or has some admixture of $R_{\perp}$ paths, in terms of an $R_{\perp,eff}$, as given by Eq (2).

Measurements on NbTi based cables demonstrated that the suppression of the loss was not due to the bulk resistivity of the core – the loss was quite similar whether the core was stainless steel, Ti, or kapton. In fact, the results suggested that the metallic cores were "insulating" (or anyway high enough that loss from $R_{\perp}$ associated paths were immeasurable), perhaps due to the expected native oxide coating. The losses for these cables were then due to $R_{//}$-associated current paths, even in the perpendicular orientation. In the case, however, of partial width cores, the losses were again dominated by the $R_{\perp}$-associated current paths, but in such cases only those not covered by a core [14]. The present measurements show a similar effect for Nb_3Sn based cables. Previous measurements of Nb_3Sn based Rutherford cables with cores have shown that the $R_{//}$-associated losses present in perpendicular fields are usually negligible in Nb_3Sn cored cables. Thus, in the present case, it is likely that the extracted value of $R_{\perp,eff}$ is entirely due to $R_{\perp}$-associated paths, but only the ones not impeded (covered) by the cores. However, in the analysis that follows, the

results are discussed in terms of the effective resistance, $R_{\perp,eff}$, which can be associated with the generic term ICR.

In the present case since for some cables substantial losses are present, it is useful to extract data from both the initial slope and the loss maximum. Along those lines, the experimental $R_{\perp,eff}$ can be obtained from the reciprocal of the linear initial slope of $Q_{\perp}(f)$ hence that of $Q_t(f)$, viz. $(dQ_t/df)_{init}$. On the other hand in case $R_{\perp,eff}$ is relatively small such that $Q_t(f)$ begins to bend over and pass through a maximum within the frequency range of the experiment (see below) a fitted initial slope, $(dQ_t/df)_{init.fit}$, is also available for use.

Higher Frequency AC Loss – The Critical Frequency Method

The simultaneous generation and decay of coupling currents gives rise to a maximum in $Q_t(f)$ at a critical frequency $f_c = 1/2\pi\tau_c$ (where τ_c is the corresponding relaxation time) following a general relationship

$$Q(f) = Q_0 \frac{f/f_c}{1+(f/f_c)^2} \tag{3}$$

which applies both to strand eddy currents as well as cable- and cable-stack coupling currents. Use is made of the low-f limit of Equation (3) to obtain a value for the fitted initial slope of $Q(f)$ and hence $R_{\perp,init.fit}$.

Relationships between the individual-cable relaxation time, τ_{cab}, and the relaxation time of the cable stack, τ_{stack}, lead to f_c-based ICR values herein designated $R_{\perp,fc}$. According to Verweij [5] $R_{\perp} = (DE)2\pi f_c$ where $E = (w/t)N_c/\{(w/t) + C(N_c\text{-}1)\} = \tau_{stack}/\tau_{cab}$, $= 1/(2\pi f_c \tau_{cab})$ and $D = 2L_pC'(N^2 - 4N) = R_{\perp}\tau_{cab}$, (in Ωs) in which $(w/t)L_p$ and N are the individual-cable parameters, N_c is the number of cables in the stack, and C and C' are the numerical constants defined in [5]. With $k=2\pi(DE)$ the per-cycle loss is given by

$$Q_{\perp}(f) = \left(\frac{\pi^2}{30}\right)\left(\frac{w}{t}\right)L_p B_m^2 N^2 \left(\frac{1}{k}\right)\left(\frac{f/f_c}{1+(f/f_c)^2}\right) \tag{4}$$

whose maximum value Q_{max} or $Q_{\perp}(f_c)$) is independent of f_c. A previous application of this critical-frequency method to uncored Nb_3Sn Rutherford cables is described in [15].

RESULTS OF THE MAGNETIC MEASUREMENTS

The results of the magnetic AC loss measurements are shown in Figures 1 and 2 fitted to Equation (4) of the form $Q = Q_h + Q_0(f/f_c)\{1/(1+(f/f_c))\} + Rf$, in which a common intercept, $Q_h = 4.95\text{x}10^4$ J/m^3, was obtained from the accompanying set of calorimetric measurements, $Q_0 = (44.6\text{-}47.3)\text{x}10^4$ J/m^3 , and $R = 20\text{x}10^4$ J.s/m^3. The small base-line slope, R (~1% in the initial slope for Cables 3, 4, and 5), was included to improve the fit to the data beyond f_c. It suggests the possible existence of a second maximum in $Q_t(f)$ well beyond the range of the present equipment, cf. [15].

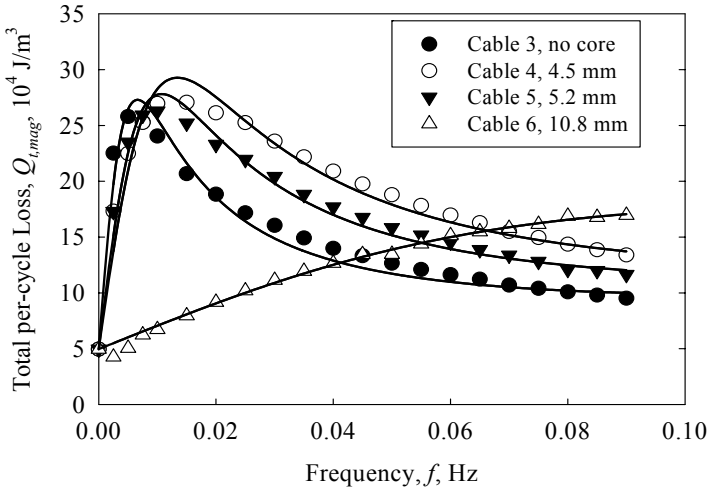

FIGURE 1. Magnetically measured loss at an AC field amplitude B_m = 400 mT

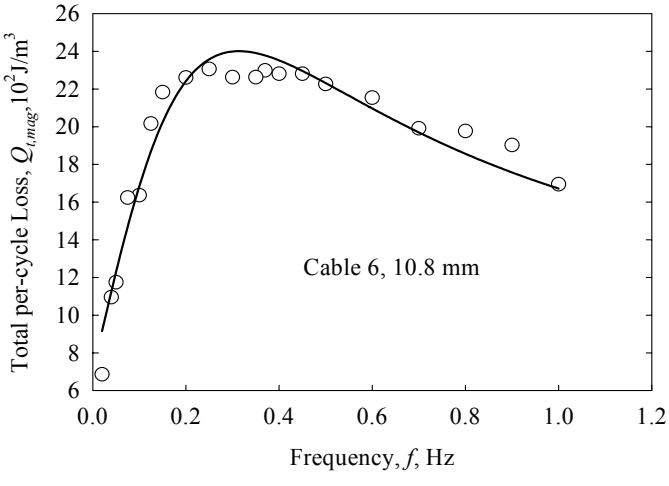

FIGURE 2. Magnetically measured loss at an AC field amplitude B_m = 50 mT

TABLE 2. Summary of the Magnetically Measured Interstrand Contact Resistances

OSU Cable No.	Core width mm	$R_\perp$ init.[a] μΩ	$R_\perp$ init.fit[b] μΩ	f_c mHz	$R_\perp$ from f_c μΩ	$<R_\perp>_{AV.}$ μΩ
3	NC	0.24	0.25	6.6	0.15	**0.21**
4	4.5	0.34	0.47	13.3	0.30	**0.37**
5	5.2	0.34	0.40	10.6	0.25	**0.33**
6	10.8	7.89	8.77	*[109]*[c] 310[d]	*[2.47]*[c] 7.02[d]	**7.90**

a) From linear fit to the raw initial data, (b) From the initial slope of the Eqn.(4)-fitted $Q_t(f)$, hence Q_{max}/f_c (c) For Cable 6, f_c is out of the frequency range of the standard experiment, (d) Extended-frequency-range result (Figure 2)

The results of the measurements in terms of the measured FO $R_{\perp,eff.}$s are summarized in Table 2. In it we notice that the introduction of narrow cores (4.5 and 5.2 mm wide in the as-wound cable) produce in the present case barely a doubling of the uncored $R_{\perp,eff.}$. Only after the inclusion of a much wider core in the present class of cables do we find $R_{\perp,eff.}$ increasing to about 8 μΩ and approaching the acceptable 10-20 μΩ range.

CONCLUDING DISCUSSION

The Uncored Cable

The uncored $R_{\perp,eff.}$ = 0.21 μΩ agrees well with several previous results obtained under a collaboration with the Lawrence Berkeley National Laboratory (LBNL) viz.: 0.24 μΩ [10] and 0.16, 0.30, 0.36 μΩ although some higher values were also obtained depending on the cable's pre-heat-treatment condition [6][16]. The result also compares well with the 0.4 μΩ obtained on a series of FNAL cables, insulated heat treated and impregnated under various conditions [15].

The Cored Cables

Previous studies of LBNL-wound Nb_3Sn cables with full-width cores yielded $R_{\perp,eff.}$ values of 23, 53, and 78 μΩ [9][10] . As for previous variable-width-core results we turn to study of LBNL-wound stabrite-coated cables. These LHC-type cables, wound to a 1.2-1.25° keystone angle and compacted to 81-98% (average 90% [5]) had cores that covered zero, 20%, 50%, 75%, and 100% of the available cable width. Measurements of the 170°C-cured cables yielded $R_{\perp,eff.}$s that increased monotonically from 2.53 to 123 μΩ. These results stimulated the winding and measurement of the present variable-core-width Nb_3Sn cables. But unlike those of the earlier measurements the present $R_{\perp,eff.}$s did not increase monotonically with core width, nore did the intended full-width core result in an expected $R_{\perp,eff.}$ in the 50-100 μΩ range. The explanation has to do with the locations and effective widths of the cores both of which were studied using scanning electron microscopy (SEM). The numerical results are summarized in Table 3.

TABLE 3. Location and Condition of the Cable Cores as Determined by SEM.

OSU Cable No.	Initial core width[a] mm	Final core width[b] mm	Distance from edge-1, mm	Distance from edge-2, mm	Condition of the core
3	No core	--	--	--	--
4	4.5	4.0	4.75	6.01	Fairly well centered
5	5.2	5.1	0.95[c]	8.27	Shifted to one side of the center-line -- curled at one edge
6	10.8	9.6	0.93[c]	3.93	Off-center but covering the center-line

(a) From cores extracted from unreacted cables, (b) Measured on cables after compaction and RHT, (c) In Cables 5 and 6 one edge of the core is wedged between an outer pair of 1 mm. diam. strands

These data and the accompanying SEM micrographs (not reproduced here) embody the following information: (1) Only Cable 4 has a well-centered core; those of the other cables were shifted all the way across to one edge leaving a large fraction of the surface exposed. (2) The edge puckering of Cable 5's core, by reducing its effective width, is partly responsible for its $R_{\perp,eff.}$ being less than that of Cable 4. (3) Undulation of the core's cross-section as it follows the curves of the nested strands causes it to shrink below its nominal width such that even the widest core did not extend from edge to edge. (4) Partly for this reason the core of Cable 6 covers only 77% of the 12.2 mm (I.D.) available cable width. Based on [5] a coverage increase of from 75% to 100% could result in a four-fold increase in $R_{\perp,eff.}$ -- to about 32 μΩ in this case. Because of the sensitivity of loss to the distributions of R⊥ across the width of the cable (Ref [2], page 84, also [14]), an even greater increase would accompany the shift of the core to the center of the cable and bring its $R_{\perp,eff.}$ more into line with previously measured values [9][10].

ACKNOWLEDGEMENTS

The cables were wound at FNAL by A. Rusy. B. Bianchi, also at FNAL, assisted with compacting and heat treating the OSU-mounted cable packs. Further compaction prior to impregnation was performed at OSU by L. Barnhart. J. Yue (Hyper Tech Research Ltd) performed the vacuum impregnation and curing of the CTD-101 resin insulation. SEM and core-position measurements were performed at OSU by V. Nazareth. The US Department of Energy, Division of High Energy Physics, funded the research at FNAL and OSU, in the latter case under grant No. DE-FG02-95ER40900.

REFERENCES

[1] Krempasky, L. and Schmidt, C., *Physica C* **310** 327-334 (1998)
[2] Verweij, A.P., *Ph.D. Thesis*, University of Twente Press, 1995
[3] Ang, Z., Bejar, I., Bottura, L., et al., *IEEE Trans. Appl. Supercond*. **9** 735-741 (1999)
[4] Wake, M., Gross, D., Yamada, R., et al., *IEEE Trans. Magn.* **MAG-15** 141-142 (1979)
[5] Sumption, M.D., Collings, E.W., Scanlan, R.M., et al., *Cryogenics* **41** 733-744 (2001)
[6] Sumption, M.D., Collings, E.W., Dietderich, D.R., et al., *IEEE Trans. Appl. Supercond.* **16** 1200(2006)
[7] Sumption, Scanlan, R.M., and Collings, E.W, *IEEE Trans. Appl. Supercond.* 11 2571-2574 (2001)
[8] Sumption, M.D., Collings, E.W., Nijhuis, A., et al., Adv. Cryo. Eng. (Materials) **46** 1043-1049 (2000)
[9] Sumption, M.D., Collings, E.W., Scanlan, R.M., et al., Cryogenics **39** 1-12 (1999)
[10] Sumption, M.D., Scanlan, R.M., Illyun, Yu.A., et al., Adv. Cryo. Eng. (Materials) **50** 781-788 (2004)
[11] Verweij, A.P., den Ouden, A., Sachse, B, et al. *Adv. Cryo. Eng.(Materials)* **40** 521-527 (1994)
[12] Sytnikov, V.E., Svalov, G.G., Akopov, S.G., et al. *Cryogenics* **29**, 926-930 (1989); see also Sytnikov, V.E., and Peshkov, I.B, *Adv. Cryo. Eng. (Materials)* **40** 537-542 (1994)
[13] M.D. Sumption, E.W. Collings, R.M. Scanlan, et al., Supercond. Sci. Technol. 14 (2001) 888-897.
[14] MD. Sumption, R.M. Scanlan, and E.W. Collings, IEEE Trans. Appl. Supercond. **11** 2571 (2001).
[15] Collings, E.W., Sumption, M.D., Ambrosio, G., et al, *IEEE Trans. Appl. Supercond.* **17** 2495 (2007).
[16] Collings, E.W., Sumption, M.D., Dietderich, D.R., et al., *Adv. Cryo. Eng. (Materials)* **52** 851-858 (2006)